

Design of a cheap compact low-pass filter with wide stopband

Priyansha Bhowmik*, Tamasi Moyra

Department of Electronics and Communication Engineering, National Institute of Technology, Agartala 799046, West Tripura, India

Corresponding Author Email: priyansha.bhowmik@gmail.com

Received: 20 January 2018

Accepted: 10 April 2018

Keywords:

low pass filter, wide stopband, hair-pin resonator, open-stubs

ABSTRACT

In these work, a cheap and compact Low-Pass filter (LPF) with wide stopband is designed using modified hair-pin resonator. The first transmission zero is obtained from the transfer function (TF) analysis of the hair-pin resonator. Further, open stubs are added to widen the stopband. An approximate LC equivalent circuit of the proposed structure is derived and the response is in accord with simulated result. A prototype of the proposed LPF is fabricated on FR4 substrate. The proposed LPF has -3 dB cut-off frequency at 1.1 GHz with wide stopband ranging from 1.6 GHz to 11.5 GHz. The size occupied by the proposed LPF is 15.8 mm x 14.3 mm. In the passband region, the insertion loss is -0.3 dB and return loss is better than -25 dB. The proposed LPF is measured and there is a good agreement between the simulated and measured results.

1. INTRODUCTION

Low-Pass Filter plays a dynamic role in suppressing spurious response of a circuit. The primary problem of designing a Low-Pass Filter (LPF) is the size of the circuit. Compared to other RF front-end components LPF occupies a larger area. In addition, wide stopband and high attenuation LPF is desirable especially in downconverter mixer, to pass the Intermediate Frequency (IF) and rejects Local Oscillator (LO), Radio Frequency (RF) and Image Frequency.

Lately, cheap, compact size and wide stopband LPF has become the research interest. To achieve sharp rejection, the order of the filter is increased, which results in higher insertion loss and enormous size [2]. Due to the large size occupied, an increase in capacitance subsequently shifts the attenuation pole close to the passband resulting in sharp rejection but provides a small stopband region. To increase the stopband different Defected Ground Structure (DGS) structure are studied [3-5]. DGS demonstrates a stopband in certain frequency band but degrades the passband performance. Alternatively, a hairpin resonator unit provides very limited stopband and occupies larger size [6-8]. In [9], to extend the stopband, a band-stop structure is embedded within a stepped impedance LPF, which suppresses the harmonics till certain extent. To provide a compact LPF, Complementary split-ring resonator (CSRR) was used [10], however, the stopband was narrow with degraded passband performance. For better suppression in the stopband, resonating patches are used [11-19]. In [11, 12] the use of resonating patches widened the stopband at the cost of suppression in stopband. In [13-15] wide stopband is accomplished due to addition of multiple stub, resulting in an increase in size. Use of multiple stub in LPF [16] accomplishes sharp roll off, but increased the size and degraded the stopband performance. In [17] wideband suppression is achieved by putting three resonators, which results in increase in size. In [18] L-C resonator was

implemented using open stub to create transmission zero, the performance was satisfactory but the size was large compared to other circuits. In [19], a low cost LPF (using dielectric substrate FR4) was proposed, but the suppression in stopband was unsatisfactory. In [20-22], resonator and open-stub was used in LPF to achieve wide stopband, but the circuit size was enhanced.

In this work, by using hair-pin resonator and open stubs a cheap, compact LPF with wide stopband is proposed. A chronological design methodology of the proposed LPF is presented in Section-2. The hair pin resonator with a resonating patch provides the first Transmission zero (TZ) at 1.8 GHz. The proposed LC equivalent circuit of the modified hair-pin resonator is in accordance with the EM simulated result. To further enhance the stopband, four open-stubs are used. The proposed LC model of the final LPF structure is derived and compared with the EM simulated result. The prototype of the proposed LPF is developed in FR4 substrate. The measured and EM simulated results of the proposed LPF are in good agreement. The passband insertion loss is -0.3 dB and return loss is better than -25 dB whereas, the suppression in stopband is more than -20 dB.

2. DESIGN METHODOLOGY

This section presents the design methodology of the proposed LPF. The first part describes modelling of the hair pin resonator to achieve first transmission zero, later the passband response is improved by adding step discontinuity. The second part describes the usage of asymmetrical stub to widen the stopband.

2.1 Hair-pin resonator with resonating patch

Fig. 1(a) shows the layout of the proposed hair-pin resonator,

which consists of a coupled line terminated with a patch resonator. The size of the patch resonator determines the first transmission zero (closest to the 3dB cut-off) of the LPF. In the proposed structure, the conventional hair pin resonator is modified by putting a resonating patch at the top with inset feed technique to make the structure compact and efficient.

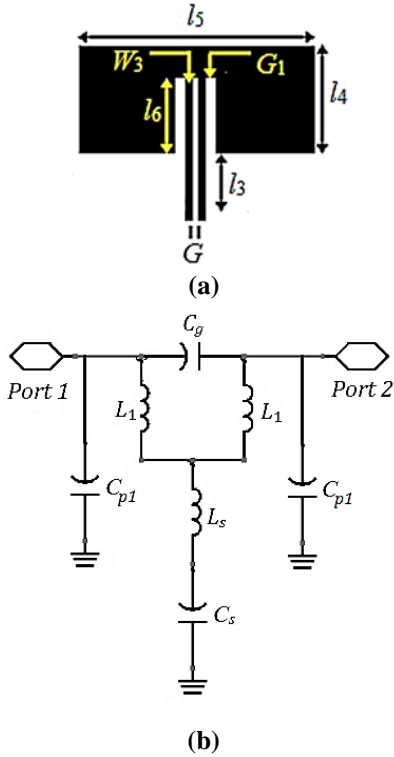


Figure 1 (a). Layout of the modified hair pin resonator and (b) LC circuit of proposed hair-pin resonator

The capacitance between the coupled lines of inductance L_1 is denoted by C_g and the parasitic capacitance is C_{p1} . The inductance and capacitance resulting from the open stub is denoted as L_s and C_s respectively. The coupled lines are viewed as π -type circuit with a LC resonator (open stub) in the middle. The equivalent circuit of the modified hair-pin resonator is modelled as shown in Fig. 1(b). The parameters for coupled lines are extracted using the equation given in [22]. The open stub is visualised as a patch resonator with its feeding position at l_6 . The LC parameter of the patch resonator are extracted using the following relation [23]:

$$l_{\text{eff}} = l_4 + \frac{0.412h(\epsilon_{\text{eff}} + 0.3) \left(\frac{l_5}{h} + 0.264 \right)}{(\epsilon_{\text{eff}} - 0.258) \left(\frac{l_5}{h} + 0.8 \right)}$$

$$C_s = \frac{\epsilon l_{\text{eff}} l_5}{2h \left(\cos \left(\frac{\pi l_6}{l_4} \right) \right)^2}$$

$$L_s = \frac{1}{(2\pi f)^2 C_s}$$

where, l_{eff} - effective length, ϵ_{eff} - effective dielectric constant, h - substrate height and $\epsilon = \epsilon_0 \epsilon_r$

The dimensions of the proposed hair-pin resonator (Fig. 1(a)) is tabulated in Table 1. The lumped parameter of the proposed hair-pin resonator is tabularised in Table 2.

Table 1. Dimensions of Fig. 1(a) in mm

Length	l_3	l_4	l_5	l_6
Value	3.9	7	15.4	4.9
Width	W_3	G	G_1	
Value	0.4	0.4	0.8	

Table 2. LC Parameters of circuit shown in Fig. 1(b)

Parameter	C_g (pF)	C_{p1} (pF)	L_1 (nH)	L_s (nH)	C_s (pF)
Calculated	0.12	0.19	2.32	1.78	4.39

As viewed in Fig. 1(b) C_g and L_1 forms a delta circuit. The delta circuit is converted to star circuit (delta-star transformation), which leads to a T-circuit. From the simplified circuit of hair-pin resonator, the transfer function (TF) of the circuit is obtained as the relation described below. From the TF, the transmission zero of the LPF is obtained. The S-parameter response in Fig. 2 shows unsatisfactory passband response.

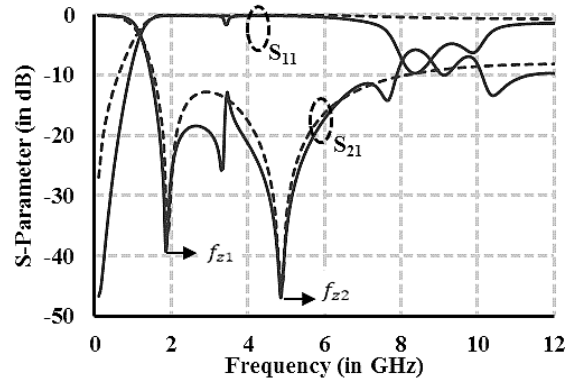


Figure 2. Comparison of EM simulated (bold lines) and LC circuit simulated (dotted lines)

TF

$$= \frac{1 + s^2(2C_g L_1 + C_s L_s) + s^4 C_g C_s L_1 (L_1)}{1 + s^2(C_s L_s + L_1(2C_g + 2C_{p1} + C_s)) + s^4 C_s L_1 (C_g L_1 +$$

$$f_{z1} = \frac{\sqrt{4L_1^2(C_g^2 + 2C_g C_{p1} + C_{p1}^2) + 2C_s L_1 L_s (C_s - 2C_g - 2C_{p1})}}{4\pi(C_s L_1^2(C_g + C_{p1}) + 2C_s)}$$

$$f_{z2} = \frac{\sqrt{4L_1^2(C_g^2 + 2C_g C_{p1} + C_{p1}^2) - 4C_s L_1 L_s (C_g + C_{p1}) + C_s^2 L_s}}{4\pi(C_s L_1^2(C_g + C_{p1}) + 2C_s)}$$

To enhance the passband response a stepped impedance line has been created as shown in Fig. 3(a). The resulting equivalent circuit for step discontinuity is shown in Fig. 3(b). The lumped elements are calculated using [1]. Here L_{D1} and L_{D2} is the additional inductance created in TL l_1 and l_2 length respectively, due to the step discontinuity. Whereas, C_D is the capacitance created due to fringing effect in the step discontinuity. A transmission pole is created due to insertion

of step discontinuity in the width of the microstrip line as shown in Fig. 3(c). The dimensions of step discontinuity are tabulated in Table 3.

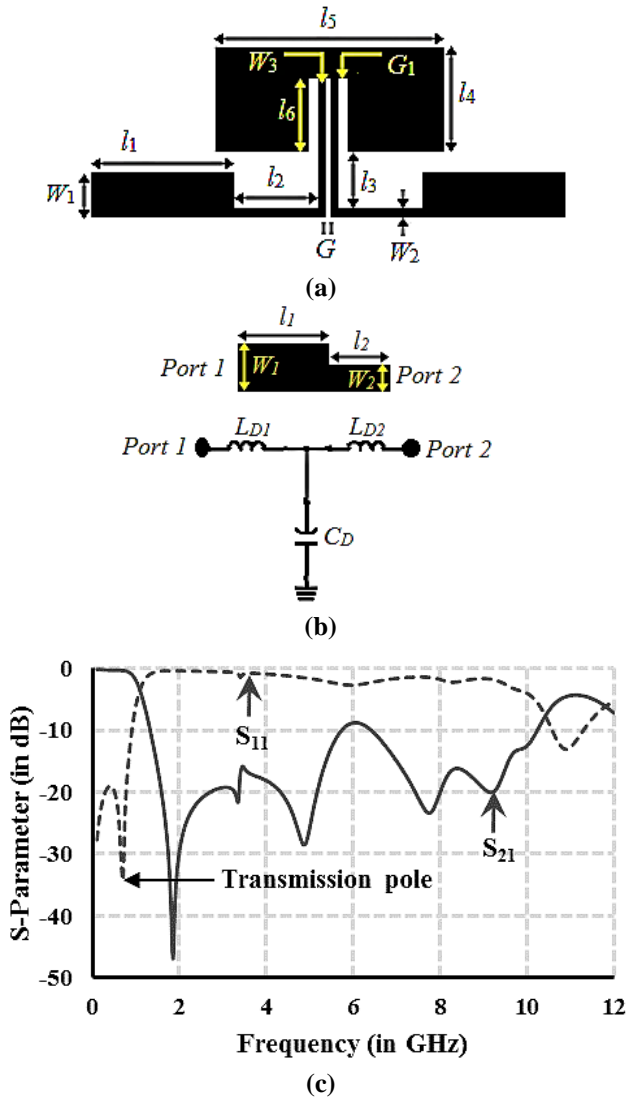


Figure 3. (a) Structure of LPF on adding of step discontinuity, (b) T-circuit for step discontinuity and (c) EM simulated S-Parameter for Fig. 3(a)

Table 3. Dimensions of the step discontinuity

Length	l_1	l_2	W_1	W_2
Value	9.5	5.8	3	0.5

2.2 Use of asymmetrical open-circuited Stub

The stop-band response of Fig. 3(c) is not wide. To widen the stopband of the LPF, open stubs are added. Fig. 4(a) shows the layout of the structure after adding symmetrical stubs and the response is observed in Fig. 4(b). It is observed that the stopband has been widened to approx. 7.5 GHz. To further extend the stopband in higher frequency, the size of the stub needs to be reduced. Hence, asymmetrical stubs are used as shown in Fig. 4(c). The dimensions of the stubs are tabularized in Table 4.

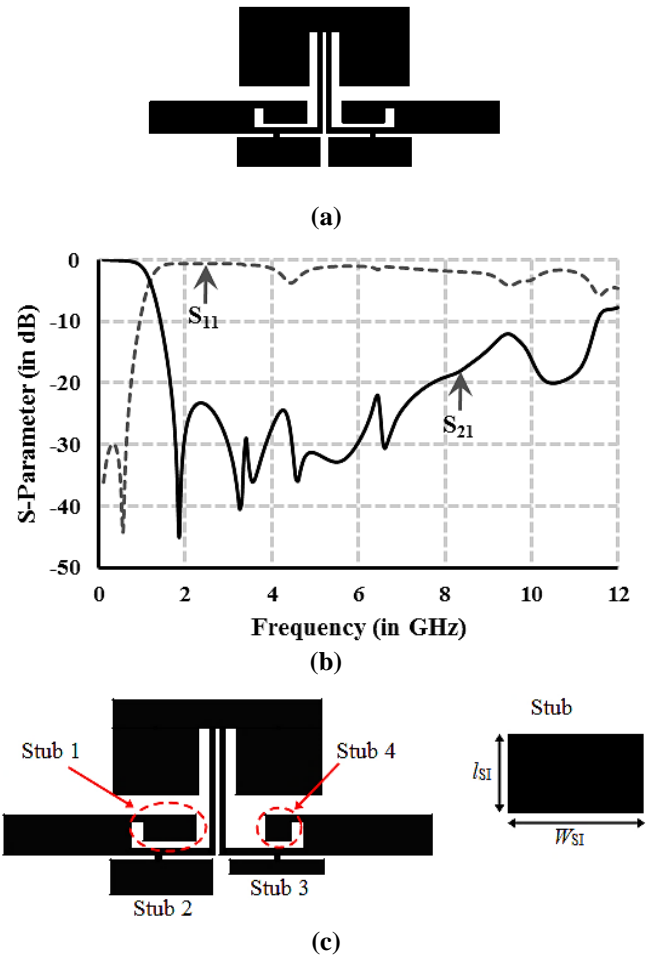


Figure 4. (a) LPF with symmetrical stub, (b) EM Simulated response of LPF with symmetrical stub and (c) Layout of the compact filter

Table 4. Dimensions (mm) of the stub incorporated in Fig. 4(c)

Length	l_{S1}	l_{S2}	l_{S3}	l_{S4}
Value	3.9	2.5	1	1.9
Width	W_{S1}	W_{S2}	W_{S3}	W_{S4}
Value	1.9	7	7	1.9

The open stub is viewed as series LC resonator. Therefore, input impedance is obtained as $Z_{in,I} = j\omega L_{SI} + 1/j\omega C_{SI}$ ($I=1, 2, 3$ and 4), and at $Z_{in,I}=0$ the circuit resonates. The input impedance of the open stubs is shown in Fig. 5.

From Fig. 5 it is concluded that due to the addition of reduced size stub the stopband is widened. For simplicity in understanding, the LC equivalent circuit of the proposed filter is described in Fig. 6. In the LC circuit, L_4 is the inductance due to step discontinuity, whereas L_2 and L_3 is the total inductance due to step discontinuity and inductance of the thin microstrip line. C_3 is the capacitance due to fringing field resulting from the step discontinuity. C_{p2} is the parasitic capacitance of the thin width TL. L_{S1} and C_{S1} represent the series inductance and capacitance of the stub I (where $I=1$ to 4).

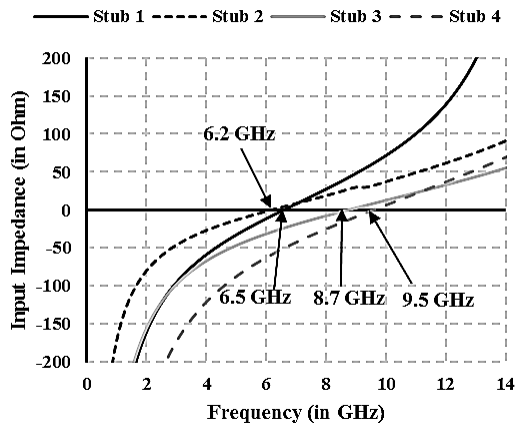


Figure 5. EM simulated Input impedance of the open stubs

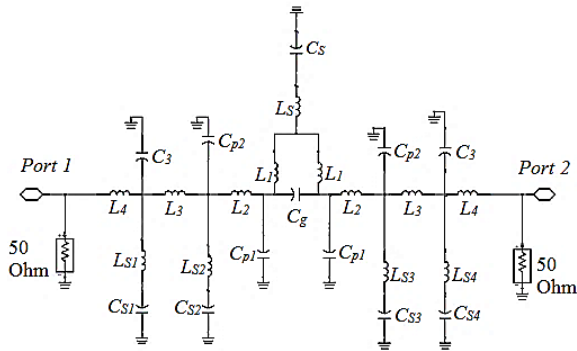


Figure 6. LC Equivalent circuit of the proposed low pass filter

Table 5. Calculated and optimised values of the lumped equivalent circuit parameters

Parameter	C_s	C_{s1}	C_{s2}	C_{s3}
Value	4.4 pF	0.47 pF	1.2 pF	1.01 pF
Parameter	C_{s4}	C_{p1}	C_{p2}	C_3
Value	0.33 pF	0.15 pF	1 pF	0.97 pF
Parameter	C_g	L_1	L_2	L_3
Value	0.145 pF	2.6 nH	5.3 nH	0.6 nH
Parameter	L_4	L_{s1}	L_{s2}	L_{s3}
Value	0.45 nH	1.2 nH	0.638 nH	0.433 nH
Parameter	L_{s4}	L_s		
Value	0.61 nH	1.9 nH		

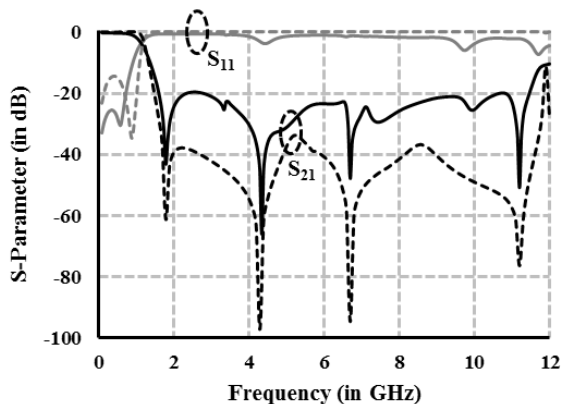


Figure 7. Comparison of EM wave simulated (bold lines) and circuit simulated (dotted lines)

The parameters are extracted using the methodology described in [1]. The calculated values are optimised using ADS and tabulated in Table 5. A comparison of LC equivalent circuit and simulated response is shown in Fig. 7. It is observed that the LC equivalent circuit has better response compared to simulated, since the lumped elements are in ideal condition, whereas signals in microstrip lines suffers due to lossy substrate.

3. RESULTS AND DISCUSSION

The proposed low pass filter is designed and simulated using MoM's based Zeland IE3D-14 software. To verify the simulated circuit a prototype is modelled on FR4 substrate (dielectric (ϵ_r) - 4.4, substrate height (h) - 1.6 mm and loss tangent ($\tan \delta$) - 0.002). The prototype is shown in Fig. 8.

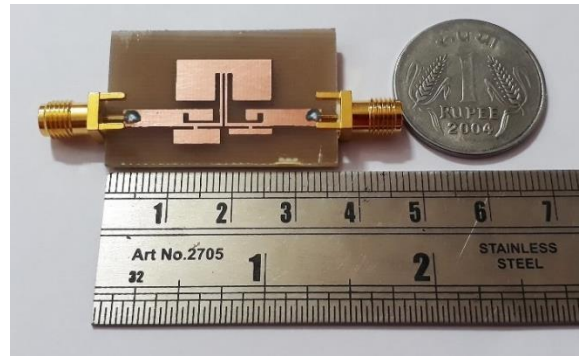
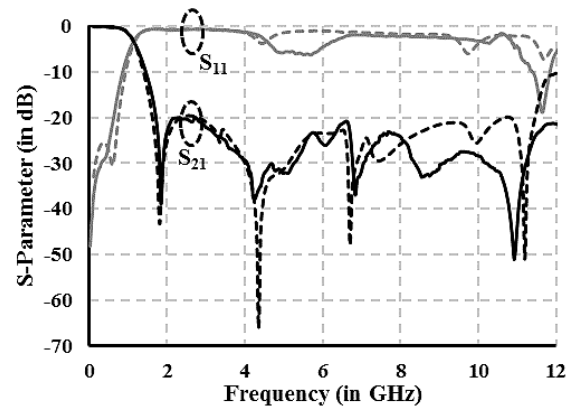
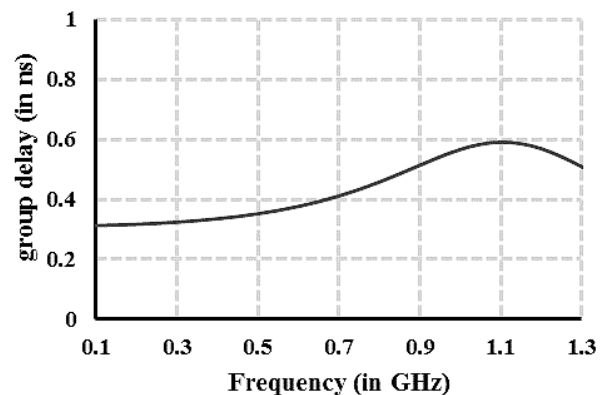


Figure 8. Prototype of the proposed low pass filter



(a)



(b)

Figure 9 (a). comparison of EM simulated (dotted line) and measured (bold line) response and (b) group delay

The comparison of simulated and measured output is shown in Fig. 9(a). As viewed from Fig. 9(a) the 3-dB cut-off frequency is 1.1 GHz. It has a wide stopband ranging from 1.60 GHz to 11.45 GHz with suppression level more than -20 dB. In the passband region, the insertion loss is less than 0.3 dB and return loss is better than 25 dB. Fig. 9(b) shows the group delay of the LPF in the passband region. The group delay of the LPF ranges from 0.3 ns to 0.6 ns, exhibiting linearity in the passband. A comparison of the proposed work

with the existing work is shown in Table 6, where RSB is the relative stop bandwidth.

$$RSB = \frac{2(f_u - f_l)}{(f_u + f_l)}$$

where, f_u =upper stopband,
 f_l =lower stopband

Table 6. Comparison of proposed work with the existing LPF

Work	ϵ_r, h (mm), $\tan\delta$	f_c (GHz)	Relative Stop Bandwidth (RSB)	Stopband Suppression (dB)	Normalized Size (λ_g^2)	Passband Insertion loss (dB)	Passband Return Loss (dB)	Group delay (ns)
[12]	3.5, 0.508, 0.0018	1.8	1.58	15	0.09×0.11	0.5	10	-
[15]	3.365, 0.508, 0.0033	1	1.57	24	0.09×0.136	0.3	20	0.75-1.5
[18]	2.2, 0.508, 0.0009	2	1.6	21	0.087×0.17	0.15	20	-
[19]	4.4, 0.6, 0.02	0.9	1.582	17	0.069×0.087	0.4	14	-
[20]	2.2, 0.508, 0.0009	2.68	1.5	20	0.164×0.157	0.12	18.5	0.2-0.62
[21]	4.4, 0.8, 0.02	2.44	1.39	22	0.257×0.148	0.62	17.74	0.3-1
[22]	3.5, 0.508, 0.0018	2.2	1.26	30	0.16×0.17	-	-	-
This Work	4.4, 1.6, 0.02	1.1	1.52	20	0.11×0.12	0.3	25	0.3-0.6

The substrate loss tangent has greater impact on the stopband performance of the LPF. The LPF of [12, 15, 18, 20, 22] uses costly substrate with low loss tangent compared to the proposed work. The proposed work has better relative stop bandwidth (RSB) than [20, 21 and 22] and better stopband suppression than [12 and 19]. With respect to size occupied, the proposed LPF is compact compared to [18, 20, 21 and 22]. The group delay of the proposed LPF is low compared to [15, 20 and 21] and linear which makes it suitable for practical application.

4. CONCLUSION

In this work, a compact LPF is proposed using modified hair-pin resonator. The LPF has wide stopband and is developed over a cheap substrate. The 3-dB cut-off frequency of the LPF is 1.1 GHz. The measured result of the prototype shows good agreement with EM simulated and circuit simulated results. The passband insertion loss is -0.3 dB and the suppression in stopband is -20 dB. In addition, low group delay provides an extra advantage for usage in practical microwave circuits.

ACKNOWLEDGMENTS

The authors want to acknowledge Mr. Lakhindar Murmu and Mr. Amit Bage of ISM Dhanbad for extending their help in the completion of the project.

REFERENCES

[1] Hong JS. (2011). Microstrip filters for RF/microwave applications, 2nd ed. Wiley, New York.

[2] Tu WH, Chang K. (2005). Compact microstrip low-pass filter with sharp rejection. *IEEE Microwave and Wireless Components Lett.* 15(6): 404-406.

[3] Ting SW, Tam KW, Martins RP. (2006). Miniaturized microstrip low pass filter with wide stopband using double equilateral u-shaped defected ground structure. *IEEE Microwave and Wireless Components Lett.* 16(5): 240-242.

[4] Faraghi A, Ojaroudi M, Ghadimi N. (2014). Compact microstrip low-pass filter with sharp selection characteristics using triple novel defected structures for UWB Applications. *Microwave and Optical Technology Letters* 56(4): 1007-1010.

[5] Verma AK, Kumar A. (2011). Synthesis of microstrip lowpass filter using defected ground structures. *IET Microw. Antennas Propag* 5(12): 1431-1439.

[6] Luo S, Zhu L, Sun S. (2008). Stopband-expanded low-pass filters using microstrip coupled-line hairpin units. *IEEE Microwave and Wireless Components Letters* 18(8): 506-508.

[7] Liang L, Liu Y, Li J, Li S, Yu C, Wu Y, Su M. (2013). A novel wide-stopband band stop filter with sharp-rejection characteristic and analytical theory. *PIER C* 40: 143-158.

[8] Yang MH, Xu J, Zhao Q. et. al. (2010). Compact, broad-stopband lowpass filters using sirs-loaded circular hairpin resonators. *Pier* 102: 95-106.

[9] He Q, Liu C. (2009). A novel low-pass filter with an embedded band-stop structure for improved stop-band characteristics. *IEEE Microwave and Wireless Components Letters* 19(10): 629-631.

[10] Xiao M, Sun G, Li X. (2015). A lowpass filter with compact size and sharp roll-off. *IEEE Microwave and Wireless Components Letters* 25(12): 790-792.

[11] Ge L, Wang JP, Guo YX. (2010). Compact microstrip lowpass filter with ultra-wide stopband. *Electronics Letters* 46(10): 689- 691.

- [12] Li Q, Zhang Y, Fan Y. (2015). Compact ultra-wide stopband low pass filter using multimode resonators. *Electronics Letters* 51(14): 1084–1085.
- [13] Abdipour AS, Abdipour AR, Lotfi S. (2015). A lowpass filter with sharp roll-off and high relative stopband bandwidth using asymmetric high-low impedance patches. *Radioengineering* 24(3): 712-716.
- [14] Hayati M, Gholami M, Vaziri HS. et al. (2015). Design of microstrip lowpass filter with wide stopband and sharp roll-off using hexangular shaped resonator. *Electronics Letters*. 51(1): 69–71.
- [15] Chen CJ, Sung CH, Su YD. (2015). A multi-stub lowpass filter. *IEEE Microwave and Wireless Components Letters* 25(8): 1-3.
- [16] Mousavi SMH, Makki SVA, Hooshangi Sh et al. (2015). High performance LPF Structure with sharp roll-off and low VSWR. *Electronics Letters* 51(24): 2017–2019.
- [17] Hayati M, Akbari M, Salahi R. (2016). Compact microstrip lowpass filter with wide stopband and very-sharp roll-off. *Electronics Letters* 52(10): 830–831.
- [18] Jahanbakhshi M, Hayati M. (2016). Design of a compact microstrip lowpass filter with sharp roll-off using combined T shaped and L-shaped resonators. *Electronics Letters* 52(23): 1931–1933.
- [19] Xu LJ, Duan Z. (2017). Miniaturized lowpass filter with wide band rejection using modified stepped-impedance hairpin resonator. *Microwave and optical technology lett.* 59(6): 1313-1317.
- [20] Sheikhi A, Alipour A., and Abdipour A. (2017). Design of compact wide stopband microstrip low-pass filter using t-shaped resonator. *IEEE Microwave and Wireless Components Letters* 27(2): 111-113.
- [21] Rekha TK, Abdulla P, Raphika PM, et al. (2017). Compact microstrip lowpass filter with ultra-wide stopband using patch resonators and open stubs. *Progress in Electromagnetics Research C* 72: 15–28.
- [22] Li Q, Zhang Y, Li D, et al. (2017). Compact low-pass filters with deep and ultrawide stopband using tri- and quad-mode resonators. *IET Microw. Antennas Propag.* 11(5): 743-748.
- [23] Ma K, Yeo KS. (2011). New ultra-wide stopband low-pass filter using transformed radial stubs. *IEEE Transactions on Microwave Theory and Techniques* 59(3): 604-611.
- [24] Jam S, Malekpoor H. (2016). Analysis on wideband patch arrays using unequal arms with equivalent circuit model in x-band. *IEEE Antennas and Wireless Propagation Letters* 15: 1861-1864.